Structure of the Kinase Domain of an Imatinib-Resistant Abl Mutant in Complex with the Aurora Kinase Inhibitor VX-680

Matthew A. Young,[1] Neil P. Shah,[3] Luke H. Chao,[1] Markus Seeliger,[1] Zdravko V. Milanov,[4] William H. Biggs, III,[4] Daniel K. Treiber,[4] Hitesh K. Patel,[4] Patrick P. Zarrinkar,[4] David J. Lockhart,[4] Charles L. Sawyers,[3] and John Kuriyan[1,2]

[1]Departments of Molecular and Cell Biology and Chemistry, Howard Hughes Medical Institute, The University of California; [2]Physical Biosciences Division, Lawrence Berkeley National Laboratory, Berkeley, California; [3]Division of Hematology and Oncology, Department of Medicine, Howard Hughes Medical Institute, The David Geffen School of Medicine, University of California, Los Angeles, California; and [4]Ambit Biosciences, San Diego, California

Abstract

We present a high-resolution (2.0 Å) crystal structure of the catalytic domain of a mutant form of the Abl tyrosine kinase (H396P; Abl-1a numbering) that is resistant to the Abl inhibitor imatinib. The structure is determined in complex with the small-molecule inhibitor VX-680 (Vertex Pharmaceuticals, Cambridge, MA), which blocks the activity of various imatinib-resistant mutant forms of Abl, including one (T315I) that is resistant to both imatinib and BMS-354825 (dasatinib), a dual Src/Abl inhibitor that seems to be clinically effective against all other imatinib-resistant forms of BCR-Abl. VX-680 is shown to have significant inhibitory activity against BCR-Abl bearing the T315I mutation in patient-derived samples. The Abl kinase domain bound to VX-680 is not phosphorylated on the activation loop in the crystal structure but is nevertheless in an active conformation, previously unobserved for Abl and inconsistent with the binding of imatinib. The adoption of an active conformation is most likely the result of synergy between the His^{396}Pro mutation, which destabilizes the inactive conformation required for imatinib binding, and the binding of VX-680, which favors the active conformation through hydrogen bonding and steric effects. VX-680 is bound to Abl in a mode that accommodates the substitution of isoleucine for threonine at residue 315 (the "gatekeeper" position). The avoidance of the innermost cavity of the Abl kinase domain by VX-680 and the specific recognition of the active conformation explain the effectiveness of this compound against mutant forms of BCR-Abl, including those with mutations at the gatekeeper position.
(Cancer Res 2006; 66(2): 1007-14)

Introduction

c-Abl is a nonreceptor tyrosine kinase that is expressed in a wide range of cells (1). The kinase activity of c-Abl is normally kept under tight control, and the deregulation of Abl due to a chromosomal translocation event has been linked to the onset of chronic myelogenous leukemia (CML), a disease that is fatal if not treated (2–5). The anomalous "Philadelphia chromosome" has been identified in ~95% of CML patients and contains a chimeric gene, which results from the fusion of the *c-Abl* gene from chromosome 9 with the *Bcr* gene on chromosome 22, resulting in the production of the BCR-Abl protein (2, 5). BCR-Abl has deregulated and elevated tyrosine kinase activity and phosphorylates a broad range of substrates, many of which play critical roles in cellular signal transduction. The tyrosine kinase activity of BCR-Abl is a causative attribute that underlies the uncontrolled proliferation of myeloid cells in CML.

Imatinib (Gleevec, Glivec, STI-571; Novartis, Basel, Switzerland) was introduced into the clinic as a therapy for CML, based upon its ability to block cell proliferation by inhibiting the tyrosine kinase activity of BCR-Abl (6, 7). Imatinib is also useful in the treatment of forms of acute lymphoblastic leukemia that are marked by the presence of the Philadelphia chromosome (7), although responses are only transient. In addition to its ability to block BCR-Abl, imatinib also inhibits the platelet-derived growth factor (PDGF) receptor and the c-Kit receptor (7, 8). This extended specificity of imatinib underlies its efficacy in the treatment of chronic myeloproliferative diseases involving activation of the PDGF receptor (9) and gastrointestinal stromal tumors involving activation of the Kit receptor (10) but notably not in the treatment of systemic mastocytosis, which is most commonly driven by an activating D816V mutation in the activation loop of Kit.

Protein kinases are signaling switches that have evolved highly specialized mechanisms for converting between active and inactive states (11, 12). Although the active conformations of all kinases must of necessity resemble each other closely to satisfy the constraints of chemistry, the inactive states of kinases are proving to be greatly variable in conformation, providing routes for the development of specificity in kinase inhibitors. Crystallographic analysis of imatinib bound to the Abl kinase domain revealed that the drug recognizes a specific autoinhibited conformation of the protein, in which a centrally located control element, known as the activation segment, is folded in so as to mimic a peptide substrate, correlated with the movement away from the active site of a catalytically critical aspartate side chain (Fig. 1; refs. 13–15). Structural analysis of the kinase domain of the c-Kit receptor has confirmed the generality of this mode of binding of imatinib to its targets (16). The recognition of a specific inactive conformation by imatinib underlies much of its specificity for the small number of kinases that it inhibits. For example, imatinib does not inhibit c-Src (8). Although the Src family kinases are closely related in sequence to Abl within the imatinib-binding site, they adopt a distinct inactive conformation that is inconsistent with imatinib binding (13, 17, 18).

Despite the generally positive response of CML patients to treatment with imatinib, a serious problem that emerges with time is the accumulation of mutations in BCR-Abl that lead to resistance

Note: M.A. Young is currently at the Department of Biological Chemistry and the Bioinformatics Program, The University of Michigan Medical School, Ann Arbor, MI 48109.

Requests for reprints: John Kuriyan, Department of Molecular and Cell Biology, University of California at Berkeley, Barker Hall MC 3202, Berkeley, CA 94720-3202. Phone: 510-643-0137; Fax: 510-643-0159; E-mail: kuriyan@uclink.berkeley.edu.

doi:10.1158/0008-5472.CAN-05-2788

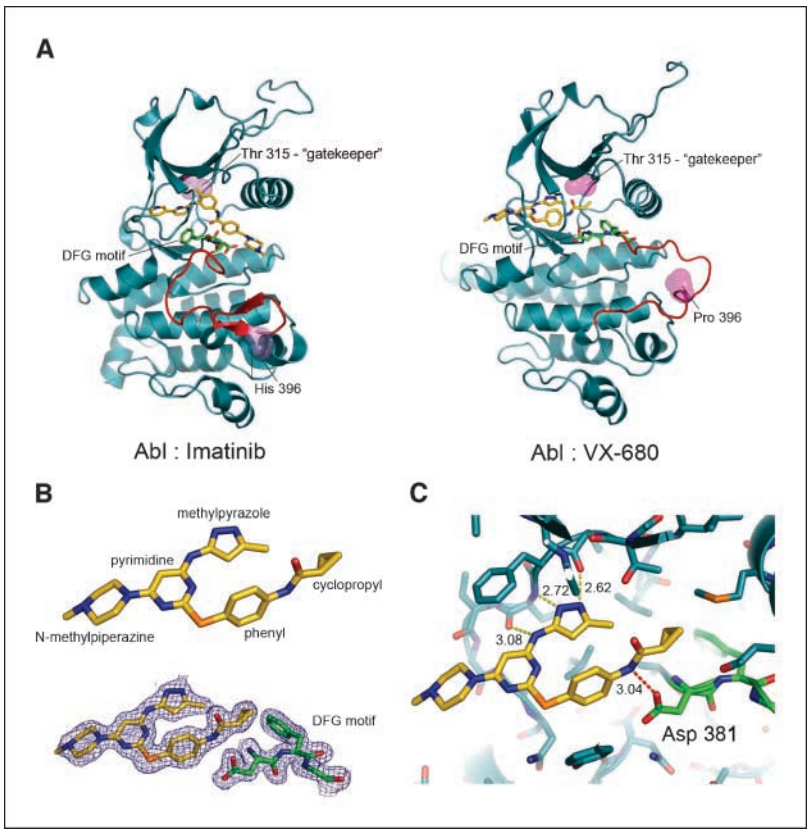

Figure 1. Structure of VX-680 complex. *A,* structure of Abl kinase domain bound to imatinib (*left*; PDB code 1OPJ; ref. 14) and VX-680 (*right*). Hydrogen atoms are not shown. *B,* chemical structure VX-680 (28) and $2F_o$-F_c electron density for VX-680 and the DFG motif contoured at 1.9σ. *C,* mode of binding of VX-680 to the Abl kinase domain. The three hydrogen bonds to the hinge region (*yellow dashed lines*) and the hydrogen bond to Asp^{381} (*red dashed line*; distances in Å).

to the drug (19). The phenomenon of resistance in these patients has been linked specifically to the acquisition of one or more of a collection of point mutations that map to the Abl kinase domain of BCR-Abl. Although some of these mutations are located close to the imatinib-binding site, most of the mutations occur at distal positions (19). A plausible mechanism for the induction of resistance by these mutations involves the destabilization of the inactive conformation, with concomitant preservation of the catalytic capabilities of the kinase domain.

An important development for the treatment of patients with resistance to imatinib is the recognition that inhibitors that can bind to both the active and inactive conformations of Abl, or that bind preferentially to the active form, provide a way to counteract the mutation-induced resistance to imatinib. A dual Src/Abl inhibitor that can bind to the active conformations of the kinase domains, BMS-354825 (now also known as dasatinib), is currently in clinical trials and is showing efficacy against most resistant forms of BCR-Abl (20, 21). Unfortunately, BMS-354825 is not effective against a mutant form of BCR-Abl in which the threonine residue at position 315 (Fig. 1) is replaced by isoleucine (T315I). The T315I mutation is predicted to represent the primary resistant point mutation in BMS-354825-treated cases (21). At present, there are no compounds in clinical development that have been documented to harbor significant activity against the T315I mutation.

The T315I mutation is one of the most common mutations found in patients undergoing imatinib therapy (19) and is responsible for ~15% of resistant cases. Thr^{315} is located in the center of the imatinib-binding site in Abl (Fig. 1). The residue at this position is referred to as the "gatekeeper" residue in protein kinases, because it separates the ATP-binding site from an internal cavity that is of variable size in different protein kinases, and the nature of the gatekeeper residue is an important determinant of inhibitor specificity (17, 22, 23). Like Abl, the Kit receptor has a threonine at the gatekeeper position, and this has been found mutated to isoleucine or to glutamate in certain patients who develop resistance to imatinib during its use as a treatment for gastrointestinal stromal tumors (24–26). Interestingly, the development of resistance to gefitinib or erlotinib in some patients being treated for lung cancer has been traced to substitution of methionine for threonine at the gatekeeper position (27) in the epidermal growth factor receptor.

Given the growing seriousness of the problem of acquired resistance to imatinib, it is important to explore the possibility of whether molecules that have been developed as inhibitors for other protein kinases and are already undergoing clinical trials might serve to inhibit imatinib-resistant forms of BCR-Abl. The compound VX-680 (Fig. 1*B*), developed as an inhibitor of the Aurora kinases (28) and currently in clinical trials, has been shown to bind a number of recurring imatinib-resistant mutant forms of Bcr-Abl, including those with mutations at the gatekeeper position (29). The identification of therapeutic leads for patients who develop insensitivity to imatinib treatment among compounds that are already being tested in the clinic may expedite the development of second line strategies for overcoming resistance; hence, there is significant interest in learning more about the properties of VX-680 as an Abl inhibitor.

In this article, we describe a crystal structure of VX-680 bound to the catalytic domain of Bcr-Abl containing a mutation ($His^{396}Pro$) that confers imatinib resistance in BCR-Abl but is inhibited by VX-680 *in vitro*. We show that this compound inhibits BCR-Abl activity in cells derived from patients carrying the T315I mutation in the kinase domain of Bcr-Abl, and that it

retains activity against purified T315I *in vitro*. Our results suggest a structural explanation for how VX-680 retains activity to mutant proteins, which no longer are sufficiently inhibited by imatinib and, in particular, why the compound is effective against the T315I mutation.

Materials and Methods

Cloning and expression. The kinase domain of human c-Abl was expressed in *Escherichia coli* (30). Briefly, a segment of c-Abl spanning residues 227 to 513 of the human c-Abl (the numbering used is that for the human Abl-1a isoform; the corresponding residue numbers in the Abl-1b isoform are increased by 19, and there are no sequence differences between the two isoforms within the kinase domain; ref. 31) was cloned into a modified pET28a *E. coli* expression vector in which the thrombin recognition sequence following the polyhistidine tag has been replaced with a tobacco etch virus (TEV) protease recognition sequence. Individual point mutations corresponding to the imatinib resistance mutants were introduced into the construct cloned into this vector using the Quickchange system (Stratagene, La Jolla, CA). To increase yields of soluble Abl, we coexpressed Abl with Yop H/Yop 2b, a potent tyrosine phosphatase from *Yersinia pestis* (32, 33) encoded by the *Yop H* gene, which was cloned into the *E. coli* expression vector pCDF Duet-1 (Novagen, Madison, WI). *E. coli* strain BL21-DE3* cells were cotransformed with 1 μL of the 248-531 c-Abl plasmid and 1 μL of YopH-pCDF duet plasmid via electroporation. Cells were grown to A_{600} of 1.0 in terrific broth containing 50 μg/mL kanamycin and 50 μg/mL streptomycin at 37°C, at which point the temperature was reduced to 18°C. Protein expression was induced with 100 μmol/L isopropyl-L-thio-B-D-galactopyranoside and continued at 18°C for 10 hours. Cells were harvested by spinning at 5,000 × *g* for 30 minutes. Pellets were resuspended in lysis buffer composed of 50 mmol/L sodium phosphate buffer (pH 7.3), 500 mmol/L NaCl, 10% glycerol, 1 mmol/L phenylmethylsulfonyl fluoride, 2 mmol/L β-ME, and flash-frozen in liquid nitrogen.

Protein purification. Protein purification was carried out at 4°C. Thawed cell pellets were lysed via three passes through an Avestin C-50 cell homogenizer under 15,000 p.s.i. pressure. During this process, the supernatant was diluted in lysis buffer to achieve a final volume of roughly 50 mL/L of cell culture. The lysate was clarified via ultracentrifugation at 40,000 × *g* for 30 minutes. The supernatant was brought to a concentration of 20 mmol/L imidazole and 500 mmol/L NaCl (as tested by conductivity) before being loaded onto a 5 mL HisTrap Ni chelating column (Amersham, Arlington Heights, IL). Protein was eluted with a 20-column volume gradient from 20 to 250 mmol/L imidazole, and fractions were pooled after identification on an SDS-PAGE gel. To remove the affinity tag, ~0.4 mg of TEV protease was added to the pooled fractions, which were dialyzed overnight against buffer containing 10 mmol/L Tris-HCl (pH 7.3), 20 mmol/L NaCl, 10% glycerol, 2 mmol/L DTT. The cleaved protein was loaded onto a high trap anion exchange column (Amersham QHP) and eluted over 20 column volumes to 250 mmol/L NaCl. Fractions containing cleaved protein were identified via SDS-PAGE and were exchanged into storage buffer [25 mM NaCl, 20 mmol/L Tris (pH 7.3), 10% glycerol, 5 mmol/L DTT] via either a S-200 or fast-desalting gel filtration column. The purified protein was concentrated to 20 mg/mL and flash-frozen in small aliquots. The typical yield of purified protein was ~7 mg/L of cell culture.

Kinase inhibition assays. Kinase activity was monitored using a continuous spectrophotometric assay as described before (34). In brief, the consumption of ATP is coupled via the pyruvate kinase/lactic dehydrogenase enzyme pair to the oxidation of NADH, which can be monitored through the decrease in absorption at 340 nm. Reactions contained 100 mmol/L Tris (pH 8), 10 mmol/L $MgCl_2$, 2.2 mmol/L ATP, 1 mmol/L phosphoenolpyruvate, 0.6 mg/mL NADH, 75 units/mL pyruvate kinase, 105 units/mL lactate dehydrogenase, and 0.5 mmol/L substrate peptide (sequence: EAIYAAPFAKKK). Reactions (75 μL) were started by adding sufficient kinase to bring the reactions to 30 nmol/L kinase concentration, and the decrease in absorbance was monitored over 30 minutes at 30°C in a microtiter plate spectrophotometer (SpectraMax). Inhibitory constants were obtained through addition of 3.75 μL drug in 100% DMSO or DMSO alone. K_i values were calculated as follows, $K_i = IC_{50} / (1 + [S]/K_d)$, where [S] = [ATP] = 2.2 mmol/L, and K_d (of ATP to Abl) = 70 μmol/L. These values were calculated assuming a K_d (ATP) of 70 μmol/L for wild type and H396P Abl kinase domain.

Crystallography. The VX-680 inhibitor, prepared as described previously (29), was dissolved in DMSO to a concentration of 20 mmol/L and added slowly to the concentrated protein (20 mg/mL), to a final concentration of 10 μmol/L. Crystals were grown by hanging drop vapor diffusion at 20°C, using a drop size of 1.4 μL. Crystals were grown in 25% w/v polyethylene glycol 1500, 100 mmol/L citric acid (pH 3.5) at 20°C and harvested after 3 to 4 days. The crystals were cryoprotected in mother liquor augmented with 33% glycerol and flash-frozen in liquid nitrogen. X-ray diffraction data were collected at beamline 8.2.1 at the Advanced Light Source in Berkeley, CA.

X-ray data were processed to 1.9 Å resolution using HKL2000 (35). The structure was determined in a straightforward manner using the program Phaser (36), as part of the CCP4 package (37), and using the structure of Abl kinase domain complexed with the small-molecule inhibitor PD173955 as the search model (protein databank code 1M52; ref. 14). Structure refinement was also straightforward, using CNS v1.1 (38) and ONO v9.0 (39). Regions of the search model that were observed or suspected to be structurally divergent from the current structure, including the activation segment (residues 381-404), were omitted from the search model and initial refinement steps to minimize model bias. Refinement variables for VX-680 were generated by performing an energy minimization of the molecular geometry using the cvff forcefield of the Discover molecular mechanics program (Accelrys) and constructing a CNS variable file by submitting the minimized conformation to the HIC-Up server (40). Force constants for rotatable torsion angles were set to 0 as the electron density clearly indicated that the *in vacuo* minimized conformation was different from the conformation bound to the protein. Continuous electron density is observed from Gly^{227} (we do not see the first two residues of the construct, which are remnants of the TEV protease recognition sequence) to Gln^{513}. An unusual aspect of the structure is that the COOH-terminal α-helix (helix αI) is extended by an extra 15 residues relative to what has been seen previously (14) for the unkinked (active) state of this helix.

Details of the data processing and refinement statistics are given in Table 1. Protein coordinates and structure factors have been deposited in the protein databank [5] with code: 2F4J.

***Ex vivo* exposure of patient cells.** After obtaining informed consent to participate in a University of California at Los Angeles Institutional Review Board–approved research blood draw protocol, peripheral blood leukocytes were obtained from a patient with lymphoid blast crisis CML that was resistant to imatinib and to BMS-354825 and purified by Ficoll-Hypaque. Sequencing of the BCR-Abl kinase domain revealed the presence of the T315I mutation. One million cells from the patient were incubated with various concentrations of VX-680 or BMS-354825 for 2 hours. Cells were then lysed in a 1% Triton lysis buffer supplemented with protease and phosphatase inhibitors. Lysates were subject to SDS-PAGE followed by immunobloting with anti-CrkL antibody (Santa Cruz Biotechnology, Santa Cruz, CA) and visualized by electrochemiluminescence.

Results and Discussion

The kinase domain of Abl H396P is in an active conformation. The structure of the kinase domain Abl H396P bound to VX-680 is shown in Fig. 1*A*. The structure is strikingly similar to the structure of the kinase domain of the Src family kinase Lck in the active conformation (41), to which it is compared in Fig. 2*A*. The conformation of the unphosphorylated activation loop, starting with the aspartate of the strictly conserved Asp-Phe-Gly (DFG) motif (Asp^{381}) and continuing to Trp^{405}, is essentially superimposable upon the conformation of the phosphorylated activation loop found

[5] http://www.rcsb.org.

Table 1. Crystallographic statistics and refinement

Data collection	
Space group	$P2_1$
Unit cell dimensions	a = 44.77 Å, b = 59.42 Å, c = 66.90 Å; α = 90.0°, β = 98.42°, γ = 90.0°
Resolution	50.0-1.9 Å*
Measured reflections	80,047
Unique reflections	24,731
Data completeness	90.4% (56%)
$I/\sigma I$	9.5 (2.1)
R_{sym}†	12.1% (53%)
Refinement	
R_{factor}/R_{free}	20.8%/24.0%
Free R test set size	1,512 reflections (5.9%)
No. protein atoms	2,327
No. heterogen atoms	33
No. solvent atoms	211
rmsd bond lengths	0.006 Å
rmsd bond angles	1.3°
rmsd B factors (main chain/side chain)	1.5 Å^2/2.4 Å^2

*Statistics for the highest resolution shell (1.9-1.97 Å) are indicated in brackets.
†$R_{sym} = \Sigma|I - \langle I \rangle|/\Sigma I$, where I is the observed intensity of a reflection, and $\langle I \rangle$ is the average intensity obtained from multiple observations of symmetry-related reflections.

in the structure of Lck (the rms deviation in Cα positions between the two structures is 0.5 Å; Fig. 2*B*). The orientation of the NH_2-terminal lobe (N-lobe) relative to the COOH-terminal lobe (C-lobe) is also very similar in the structures of Abl H396P and active Lck (Fig. 2*A*). If the two structures are first superimposed on the C-lobes, the resulting rms deviation in the N-lobes is 3.9 Å, which is reduced to 1.7 Å upon further superposition of the N-lobes.

The major difference between the structure of Abl H396P and that of wild-type Abl bound to Gleevec is in the conformation of the activation loop (Fig. 2*C*). The conformation of the DFG motif in the VX-680 complex is one that is representative of an active protein kinase, because the side chain of Asp^{381} in the DFG motif points into the active site, where it normally coordinates a Mg^{2+} ion. This is in contrast to the conformation found in the imatinib complex, in which the DFG motif has undergone a backbone crankshaft rotation that involves ~180 degrees rotations of two backbone torsion angles (ϕ of Asp^{381} and ψ of Phe^{382}). The crankshaft rotation of the DFG motif in the imatinib complex moves the side chain of Asp^{381} out of the active side, where it is replaced by the side chain of Phe^{382}. The rest of the activation loop is also rearranged significantly in the imatinib complex and, instead of being in an extended and open conformation, it folds into the main body of the kinase domain, with the central segment containing the site of phosphorylation (Tyr^{393}) mimicking a peptide substrate (Fig. 1*A* and Fig. 2*C*).

The close structural similarity between the activation loops of unphosphorylated c-Abl and phosphorylated and active Lck (Fig. 2*B*; ref. 41) offers structural evidence that the "active" state of c-Abl is a thermodynamically accessible state of the unphosphorylated protein. This is consistent with the observation that the isolated kinase domain of Abl, when removed from the regulatory domains that are found both NH_2-terminal and COOH-terminal to the kinase domain of the protein, does not require phosphorylation for activity (13). The addition of a phosphate group onto Tyr^{393} is expected to stabilize the active conformation of the activation loop. Two positively charged side chains, Arg^{362} and Arg^{384}, are poised to form salt bridges with a phosphate group on Tyr^{393} (Fig. 2*B*). In wild-type Abl, a third basic side chain that could potentially coordinate the phosphate group would be provided by His^{396} (mutated here to proline). These ion-pairing interactions are presumably important in the intact protein for overcoming the inhibitory actions of the regulatory domains.

It is straightforward to understand why the conformation adopted by Abl when bound to imatinib is not tolerated by the H396P mutation. Because of the formation of a backbone-linked structure by the proline side chain, the backbone dihedral angle ϕ of this side chain is constrained to have values near −65 degrees (42). In the Abl H396P structure, the value of ϕ for Pro^{396} is −60 degrees. In contrast, the value of ϕ for His^{396} in the wild-type Abl complex bound to imatinib is −174 degrees, a value that cannot be tolerated by proline, thus explaining why the H396P mutation leads to imatinib resistance. Importantly, the value of ϕ for the residue at the corresponding position in the structure of active Lck (Arg^{397}) is −68 degrees, which is consistent with the restriction on the proline backbone and explains why the proline substitution at this position maintains catalytic activity. Restricting the intrinsic conformational flexibility of the activation loop via this mutation may have the additional effect of facilitating crystal growth, as well formed crystals of this particular mutant are more readily grown than for wild-type Abl kinase domain.

The wild-type Abl kinase domain has been crystallized with the inhibitor PD173955, and the structure of the complex shows that the activation loop is an extended conformation that resembles the active conformation, except that the DFG motif and several of the following residues (from Asp^{381} to Gly^{390}) are flipped about the backbone with respect to the active conformation (14; Fig. 2*C*). His^{396} in the PD173955 complex is in an essentially active conformation, with the value of ϕ being −52.3 degrees. This is close enough to the value required for proline that it is likely that the H396P mutant form of Abl can readily adopt the inactive conformation seen previously in the Abl:PD173955 complex. As we discuss below, adoption of the fully active conformation by the kinase domain in the VX-680 complex is most likely a result of a hydrogen bonding interaction between VX-680 and Asp^{381}, which would favor the DFG motif being maintained in the active conformation.

Mode of binding of VX-680. VX-680 is a Y-shaped molecule, with a *N*-methyl-piperazine group forming the base or leg of the "Y," a pyrimidine group at the fork, and a methylpyrazole group at one arm and a substituted phenyl group at the other arm (Fig. 1*B*). VX-680 is bound at the ATP-binding site of the Abl kinase domain, with the *N*-methyl-piperazine group extending out of the kinase domain. The electron density for the entire VX-680 molecule and the surrounding protein side chains is very clearly resolved, leaving no ambiguity as to the mode of interaction (Fig. 1*B*).

The molecule is anchored to the kinase domain by four hydrogen bonds (Fig. 1*C*). Three of these are formed between two carbonyl groups (Glu^{316} and Met^{318}) and an amide nitrogen (Met^{318}) in the

so-called "hinge region" of the kinase and three nitrogen atoms, one in the linker between the pyrimidine group and the methylpyrazole group, and the other two in the methylpyrazole group (Fig. 1*C*). The fourth hydrogen bond is between the nitrogen of the amide group linking the phenyl group to the cyclopropyl sustituent and the side chain of the aspartate of the DFG motif (Asp^{381}). This last hydrogen bond is well formed, with an oxygen-nitrogen distance of 3.0 Å, and is likely to be the interaction that enforces the active conformation of the kinase domain when it binds to VX-680. If the kinases were to adopt the conformation seen in the PD173955 complex, the phenyl side chain of Phe^{382} of the DFG motif would abut the amide group of VX-680, which is expected to be unfavorable because it leaves the amide group without a hydrogen bonding partner. The same would be the case if the kinase domain adopted the conformation seen in the imatinib complex.

Imatinib is unusual in that it makes only one direct hydrogen bond to the hinge region, to the backbone amide nitrogen on Met^{318}. A second hydrogen bond between imatinib and the hinge region is not to the backbone of the protein but to the side-chain oxygen of Thr^{315}, at the gatekeeper position, making imatinib critically sensitive to substitutions at the gatekeeper position. Another key difference between imatinib and VX-680 is that the latter anchors itself firmly at the hinge region and engages Asp^{381} but does not penetrate nearly as deeply into the kinase domain as does imatinib. Thus, the *N*-methyl-piperazine group of VX-680 is essentially exposed to solvent, whereas the corresponding region of imatinib in the structure of the complex is barely visible from the outside (Fig. 3*A*).

One feature that is shared between the binding modes of imatinib and VX-680 is that the phosphate binding "P-loop" of the kinase (residues Lys^{247} to Val^{256}) is distorted from the β-hairpin conformation that it adopts when ATP is bound and instead folds into the active site of the kinase such that the side chain of Tyr^{253} forms hydrophobic packing interactions with the inhibitor in both cases (Fig. 3*B*). The P-loop is the site of several mutations that confer resistance to imatinib binding (19). The structural basis for the properties of these mutations is not well understood at present, but one possibility is that they destabilize the folded-in conformation of the P-loop.

Explaining the broad specificity of VX-680 and inhibition of Abl T315I. The three hydrogen bonds made by VX-680 to the polypeptide backbone of the hinge region of the kinase domain are a common feature of kinase inhibitors and are independent of the sequence of the kinase (22). Likewise, the fourth hydrogen bond made by VX-680, to the side chain of Asp^{381}, is to a strictly invariant catalytic residue. Using these four sequence-independent hydrogen bond anchors, the inhibitor makes contact with 14 side chains within the kinase domain (Fig. 3*C*). All of these, with the exception of Met^{290}, are part of the core region of the kinase domain involved in ATP binding and catalysis and are highly conserved across tyrosine and serine/threonine kinases.

VX-680 was originally developed as an Aurora kinase inhibitor, and several structures of the Aurora kinases are available, although none with an inhibitor bound (protein databank codes 1MQ4, 1MUO, 1OL5, 1OL6, and 1OL7; refs. 43–45). Using the structure of an active form of Aurora-A (1MQ4; ref. 43) as a guide, the changes in sequence around the VX-680-binding site between Abl and Aurora are indicated in Fig. 3*C*. The general pattern of residue substitution is similar to that seen when comparing the structure of c-Kit bound to imatinib (16) with that of Abl (14), where roughly half of the contact

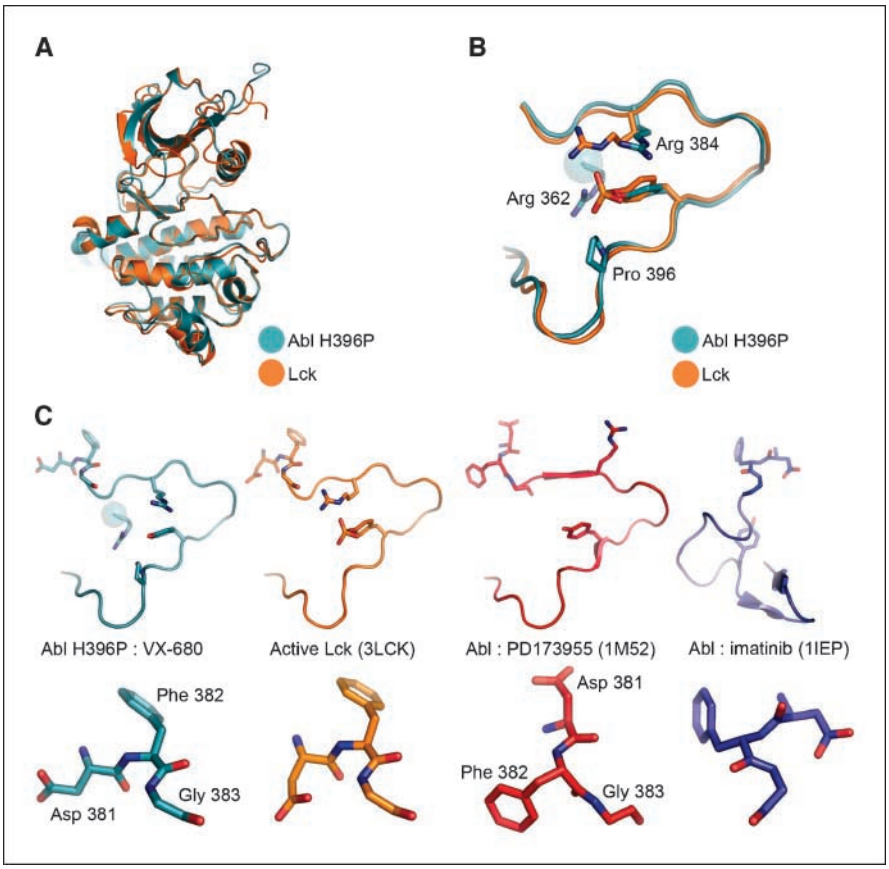

Figure 2. Comparison of VX-680 complex with other structures. *A,* superposition of the Abl:VX-680 complex (*blue*) with the structure of the active form of the Lck kinase domain (PDB code 3LCK; ref. 41; *orange*). *B,* conformation of the activation loop of Abl:VX-680 (*blue*) superimposed on the structure of the active and phosphorylated activation loop of Lck (3LCK; *orange*). *C,* active conformation of the DFG loop in the VX-680 complex (*blue*) compared with active conformation of Lck (3LCK; *orange*; ref. 41), the inactive conformation in the complex with PD173955 (*red*; 1M52; ref. 14), and inactive conformation in complex with imatinib (*dark blue*; 1OPJ; ref. 14).

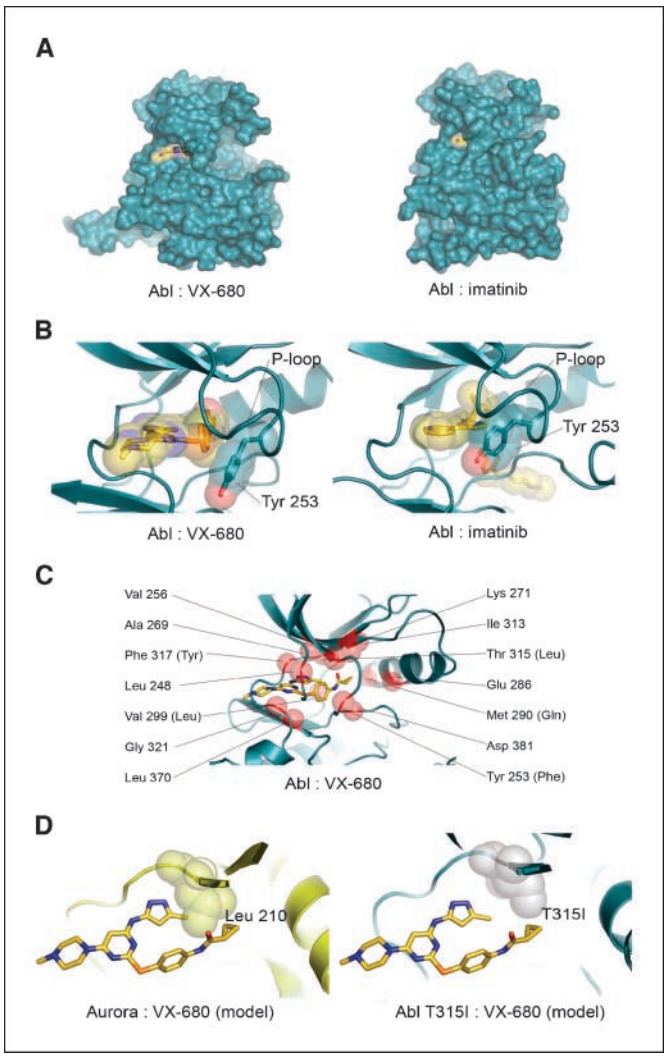

Figure 3. Mode of binding of VX-680. *A,* extent of burial of VX-680 (*left*) and imatinib (*right*). *B,* interactions between the phosphate binding loop (*P-loop*) of the kinase domain and VX-680 (*left*) and imatinib (*right*). *C,* residues that make side chain contact with VX-680 (defined as having any side-chain atom within 5.0 Å of the drug; *red spheres*). Residues in which only the Cα atom or the backbone make contact with VX-680 are not shown (except for glycine). Residues that are substituted in Aurora-A are indicated by naming the Aurora-A residue in parentheses. *D,* interaction between VX-680 and Aurora-A (*yellow*; 1MQ4; ref. 43), modeled on the basis of the Abl:VX-680 structure. The position of VX-680 within Aurora was obtained by aligning the two kinase domain on the residues of the hinge region. Leu^{210} in Aurora-A, located at the gatekeeper position, is shown with spheres for the side-chain atoms. Interaction between VX-680 and Abl (T315I; *blue*), modeled by substituting Thr^{315} in the crystal structure with isoleucine.

residues are replaced with conservative substitutions (16). Eight of 14 contact side chains are identical between Abl and Aurora, and four of the remaining six sites involve conservative substitutions (Fig. 3*C*). One of the nonconservative substitutions occurs at Met^{290} in Abl, which is replaced by glutamine in Aurora. This residue is at the periphery of the inhibitor binding site, and glutamine is not predicted to make close contact with the inhibitor.

The other nonconservative substitution in the Aurora kinase is at the gatekeeper position, where Thr^{315} in Abl is replaced by Leu^{210} in Aurora-A (Fig. 3*D*). By aligning the structures of Abl and Aurora-A on the hinge regions of the kinases, we can dock the VX-680 molecule into Aurora-A, and this reveals that the Leu^{210} side chain would be accommodated between the two arms of the "Y" of VX-680 (Fig. 3*D*; some small adjustments in side-chain conformation are required to relieve close contacts, but these should be readily accessible to the protein). In Abl, the oxygen atom of Thr^{315} side chain at the gatekeeper position makes a weak hydrogen bond to one of the nitrogens of the methylpyrazole group of VX-680 (nitrogen-oxygen distance of 3.5 Å). This nitrogen atom of VX-680 also makes a significantly stronger hydrogen bond to the carbonyl oxygen of the backbone of Glu^{316} in Abl (nitrogen to oxygen distance of 2.6 Å), and this hydrogen bond would be maintained and perhaps even strengthened upon substitution of Thr^{315} by leucine or isoleucine.

Comparison with the Aurora-A structure and simple modeling show that the side chain of isoleucine at position 315 of Abl can be accommodated within the Abl:VX-680 complex readily (Fig. 3*D*). Consistent with this, VX-680 is able to inhibit the kinase activity of the purified kinase domain of both wild-type Abl and Abl (T315I), whereas imatinib is ineffective against Abl (T315I; Fig. 4). The IC_{50} values forVX680 in the presence of 2.2 mmol/L ATP are comparable for wild-type Abl (2.2 μmol/L) and Abl (T315I; 3.7 μmol/L). These values of the IC_{50} imply that the values of the inhibitory constants (K_i) for VX-680 are 68 and 114 nmol/L, for wild-type Abl and Abl (T315I), respectively.

Inhibition of BCR-Abl/T315I in primary CML cells. To assess for the ability of VX-680 to inhibit BCR-Abl/T315I activity in primary CML cells, we exposed peripheral blood mononuclear cells from a patient known to harbor the T315I mutation to increasing concentrations of VX-680 or BMS354825 (Fig. 5). The patient had

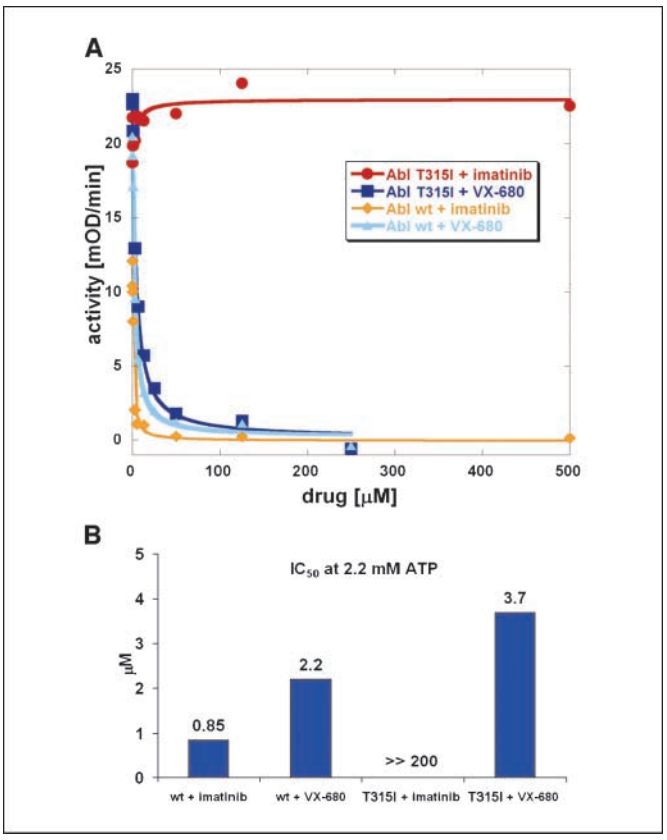

Figure 4. Inhibition of purified kinase domain of Abl by VX-680 and imatinib. *A,* T315I Abl kinase activity is shown not to be affected by imatinib, whereas VX-680 binds less tightly to wild-type Abl than T315I Abl. *B,* IC_{50} values for wild-type and T315I Abl for imatinib and VX-680.

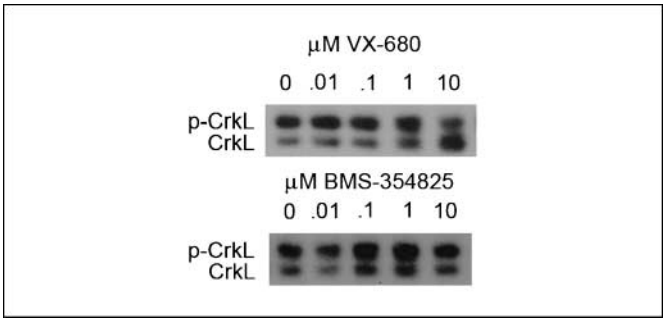

Figure 5. VX-680 inhibits BCR-Abl/T315I in primary CML cells. Exposure of peripheral blood mononuclear cells isolated from a patient known to harbor BCR-Abl/T315I to the concentrations of VX-680 or BMS-354825 followed by Western immunoblotting with a CrkL antibody. Migration of phospho-CrkL species.

developed resistance to imatinib and subsequently had no response to BMS-354825. CrkL is an adaptor protein that is phosphorylated in CML cells almost exclusively by BCR-Abl. Although concentrations up to 10 μmol/L BMS354825 failed to result in a reduction of phospho-CrkL species, a clear inhibitory effect of BCR-Abl/T315I-mediated signaling was observed with 10 μmol/L VX-680. These data are in excellent agreement with our *in vitro* and cell-based data. Although it is not yet known whether low micromolar concentrations of VX-680 can be achieved safely in humans, it is clear that concentrations of imatinib approaching 5 μmol/L can be routinely administered without significant toxicity.

Conclusions

Our primary interest in determining the structure of VX-680 bound to the Abl kinase domain was in understanding the basis for its effectiveness against mutant forms of BCR-Abl that are resistant to imatinib. We have not as yet obtained useful crystals of VX-680 bound to Abl with a mutation at the gatekeeper position (e.g., T315I), but we have succeeded in obtaining a structure of this inhibitor bound to Abl H396P, another imatinib-resistant mutant. The structure of this mutant form of the Abl kinase domain is seen to be in an active form, which mimics closely the structure of activated and phosphorylated Lck, although the activation loop of Abl is not phosphorylated in this structure. VX-680 is seen to recognize a critical element of the active form of protein kinases, by forming a hydrogen bond with the strictly conserved Asp^{381} of the DFG motif and maintaining it in an orientation close to one that is normally seen in active kinases. In contrast to imatinib, which penetrates deeply into the Abl kinase domain, VX-680 is not fully buried within the kinase domain, and is anchored to it by four hydrogen bonds to sequence-invariant elements. Comparison with the structures of the Aurora kinases reveals that all of the essential contacts between VX-680 and the protein involve highly conserved elements, explaining the broad specificity of this inhibitor. The Y-shaped structure of VX-680 engages the Abl kinase domain in such a way that close encounter with the residue at the gatekeeper position is avoided, explaining the ability of the drug to accommodate leucine (in Aurora kinases) and isolecuine (in the imatinib-resistant T315I mutant form of Abl) at the gatekeeper position. Consistent with this, we show that BCR-Abl bearing the T315I mutation from a patient-derived sample is inhibited by VX-680. These results auger well for the eventual clinical application of Abl inhibitors that are effective against commonly occurring imatimib-resistant mutations, particularly those at the gatekeeper position of the kinase domain.

Acknowledgments

Received 8/6/2005; accepted 10/5/2005.

Grant support: Burroughs-Wellcome Fund's Career Award at the Scientific Interface 1003999 (M.A.Young), Leukemia and Lymphoma Society Career Development Award for Special Fellows (N.P. Shah), and University of California at Los Angeles K12 Mentored Clinical Pharmacology Research Scholars Award (N.P. Shah).

The costs of publication of this article were defrayed in part by the payment of page charges. This article must therefore be hereby marked *advertisement* in accordance with 18 U.S.C. Section 1734 solely to indicate this fact.

We thank Marsha N. Henderson, Bhushan Nagar, Patricia Pellicena, Thomas Schindler, and Xuewu Zhang for helpful discussions and advice; Bayard Clarkson, M.D. for introducing J. Kuriyan to the challenge of inhibiting Abl kinase activity in CML; the staff of the Advanced Light Source in Berkeley, CA for excellent crystallographic support; David King for mass spectrometry; and the Ambit screening group, Miles A. Fabian, Philip T. Edeen, and Julia M. Ford.

References

1. Pendergast AM. The Abl family kinases: mechanisms of regulation and signaling. Adv Cancer Res 2002;85:51–100.
2. Clarkson B, Strife A, Wisniewski D, Lambek CL, Liu C. Chronic myelogenous leukemia as a paradigm of early cancer and possible curative strategies. Leukemia 2003;17:1211–62.
3. Wong S, Witte ON. The BCR-ABL story: bench to bedside and back. Annu Rev Immunol 2004;22:247–306.
4. Hantschel O, Superti-Furga G. Regulation of the c-Abl and Bcr-Abl tyrosine kinases. Nat Rev Mol Cell Biol 2004;5:33–44.
5. Sawyers CL, Druker B. Tyrosine kinase inhibitors in chronic myeloid leukemia. Cancer J Sci Am 1999;5:63–9.
6. Deininger M, Buchdunger E, Druker BJ. The development of imatinib as a therapeutic agent for chronic myeloid leukemia. Blood 2005;105:2640–53.
7. Druker BJ, Sawyers CL, Kantarjian H, et al. Activity of a specific inhibitor of the BCR-ABL tyrosine kinase in the blast crisis of chronic myeloid leukemia and acute lymphoblastic leukemia with the Philadelphia chromosome. N Engl J Med 2001;344:1038–42.
8. Buchdunger E, Cioffi CL, Law N, et al. Abl protein-tyrosine kinase inhibitor STI571 inhibits *in vitro* signal transduction mediated by c-kit and platelet-derived growth factor receptors. J Pharmacol Exp Ther 2000;295:139–45.
9. Apperley JF, Gardembas M, Melo JV, et al. Response to imatinib mesylate in patients with chronic myeloproliferative diseases with rearrangements of the platelet-derived growth factor receptor β. N Engl J Med 2002;347:481–7.
10. Demetri G. Targeting the molecular pathophysiology of gastrointestinal stromal tumors with imatinib. Mechanisms, successes, and challenges to rational drug development. Hematol Oncol Clin North Am 2002;16:1115–24.
11. Huse M, Kuriyan J. The conformational plasticity of protein kinases. Cell 2002;109:275–82.
12. Nolen B, Taylor S, Ghosh G. Regulation of protein kinases; controlling activity through activation segment conformation. Mol Cell 2004;15:661–75.
13. Schindler T, Bornmann W, Pellicena P, Miller WT, Clarkson B, Kuriyan J. Structural mechanism for STI-571 inhibition of abelson tyrosine kinase. Science 2000;289:1938–42.
14. Nagar B, Bornmann WG, Pellicena P, et al. Crystal structures of the kinase domain of c-Abl in complex with the small molecule inhibitors PD173955 and Imatinib (STI-571). Cancer Res 2002;62:4236–43.
15. Nagar B, Hantschel O, Young MA, et al. Structural basis for the autoinhibition of c-Abl tyrosine kinase. Cell 2003;112:859–71.
16. Mol CD, Dougan DR, Schneider TR, et al. Structural basis for the autoinhibition and STI-571 inhibition of c-Kit tyrosine kinase. J Biol Chem 2004;279:31655–63.
17. Schindler T, Sicheri F, Pico A, Gazit A, Levitzki A, Kuriyan J. Crystal structure of Hck in complex with a Src family-selective tyrosine kinase inhibitor. Mol Cell 1999;3:639–48.
18. Xu W, Doshi A, Lei M, Eck MJ, Harrison SC. Crystal structures of c-Src reveal features of its autoinhibitory mechanism. Mol Cell 1999;3:629–38.
19. Shah NP, Nicoll JM, Nagar B, et al. Multiple BCR-ABL kinase domain mutations confer polyclonal resistance to the tyrosine kinase inhibitor imatinib (STI571) in chronic phase and blast crisis chronic myeloid leukemia. Cancer Cell 2002;2:117–25.
20. Shah NP, Tran C, Lee FY, Chen P, Norris D, Sawyers CL. Overriding imatinib resistance with a novel ABL kinase inhibitor. Science 2004;305:399–401.
21. Burgess MR, Skaggs BJ, Shah NP, Lee FY, Sawyers CL. Comparative analysis of two clinically active BCR-ABL kinase inhibitors reveals the role of conformation-specific binding in resistance. Proc Natl Acad Sci U S A 2005;102:3395–400.
22. Noble ME, Endicott JA, Johnson LN. Protein kinase inhibitors: insights into drug design from structure. Science 2004;303:1800–5.
23. Liu Y, Bishop A, Witucki L, et al. Structural basis for selective inhibition of Src family kinases by PP1. Chem Biol 1999;6:671–8.

24. Tamborini E, Bonadiman L, Greco A, et al. A new mutation in the KIT ATP pocket causes acquired resistance to imatinib in a gastrointestinal stromal tumor patient. Gastroenterology 2004;127:294–9.

25. Wardelmann E, Thomas N, Merkelbach-Bruse S, et al. Acquired resistance to imatinib in gastrointestinal stromal tumours caused by multiple KIT mutations. Lancet Oncol 2005;6:249–51.

26. Debiec-Rychter M, Cools J, Dumez H, et al. Mechanisms of resistance to imatinib mesylate in gastrointestinal stromal tumors and activity of the PKC412 inhibitor against imatinib-resistant mutants. Gastroenterology 2005;128:270–9.

27. Pao W, Miller VA, Politi KA, et al. Acquired resistance of lung adenocarcinomas to gefitinib or erlotinib is associated with a second mutation in the EGFR kinase domain. PLoS Med 2005;2:e73.

28. Harrington EA, Bebbington D, Moore J, et al. VX-680, a potent and selective small-molecule inhibitor of the Aurora kinases, suppresses tumor growth *in vivo*. Nat Med 2004;10:262–7.

29. Carter TA, Wodicka LM, Shah NP, et al. Inhibition of drug-resistant mutants of ABL, KIT, and EGF receptor kinases. Proc Natl Acad Sci U S A 2005;102:11011–6.

30. Seeliger MA, Young M, Henderson MN, et al. High yield bacterial expression of active c-Abl and c-Src tyrosine kinases. Protein Sci 2005;14:3135–9.

31. Shtivelman E, Lifshitz B, Gale RP, Roe BA, Canaani E. Alternative splicing of RNAs transcribed from the human abl gene and from the bcr-abl fused gene. Cell 1986;47:277–84.

32. Guan KL, Dixon JE. Protein tyrosine phosphatase activity of an essential virulence determinant in *Yersinia*. Science 1990;249:553–6.

33. Bliska JB, Guan KL, Dixon JE, Falkow S. Tyrosine phosphate hydrolysis of host proteins by an essential *Yersinia* virulence determinant. Proc Natl Acad Sci U S A 1991;88:1187–91.

34. Barker SC, Kassel DB, Weigl D, Huang X, Luther MA, Knight WB. Characterization of pp60c-src tyrosine kinase activities using a continuous assay: autoactivation of the enzyme is an intermolecular autophosphorylation process. Biochemistry 1995;34:14843–51.

35. Otwinowski Z, Minor W. Processing of X-ray diffraction data collected in oscillation mode. Methods Enzymol 1997;276:307–26.

36. McCoy AJ, Grosse-Kunstleve RW, Storoni LC, Read RJ. Likelihood-enhanced fast translation functions. Acta Cryst 2005;D61:458–64.

37. Collaborative Computational Project N. The CCP4 suite programs for protein crystallography. Acta Cryt 1994;D50:760–3.

38. Brunger AT, Adams PD, Clore GM, et al. Crystallography and NMR system: a new software suite for macromolecular structure determination. Acta Crystallogr D Biol Crystallogr 1998;54:905–21.

39. Jones TA, Zou JY, Cowan SW, Kjeldgaard M. Improved methods for building protein models in electron density maps and the location of errors in these models. Acta Crystallogr 1991;A47:110–9.

40. Kleywegt GJaJ, TA. Databases in protein crystallography. Acta Cryst 1998;D54:1119–31 (CCP4 Proceedings).

41. Yamaguchi H, Hendrickson WA. Structural basis for activation of the human lymphocyte kinase Lck upon tyrosine phosphorylation. Nature 1996;384:484–9.

42. MacArthur MW, Thornton JW. Influence of proline residues on protein conformation. J Mol Biol 1991;218:397–412.

43. Nowakowski J, Cronin CN, Mcree DE, et al. Structures of the cancer-related Aurora-A, Fak and Epha2 protein kinases from nanovolume crystallography. Structure (Camb) 2002;10:1659–67.

44. Cheetham GM, Knegtel RM, Coll JT, et al. Crystal structure of aurora-2, an oncogenic serine/threonine kinase. J Biol Chem 2002;277:42419–22.

45. Bayliss R, Sardon T, Vernos I, Conti E. Structural basis of Aurora-A activation by TPX2 at the mitotic spindle. Mol Cell 2003;12:851–62.

Structure of the Kinase Domain of an Imatinib-Resistant Abl Mutant in Complex with the Aurora Kinase Inhibitor VX-680

Matthew A. Young, Neil P. Shah, Luke H. Chao, et al.

Cancer Res 2006;66:1007-1014.